U.S. DEPARTMENT OF COMMERCE
Peter G. Peterson, Secretary

NATIONAL OCEANIC AND ATMOSPHERIC ADMINISTRATION
Robert M. White, Administrator
ENVIRONMENTAL RESEARCH LABORATORIES
Wilmot N. Hess, Director

NOAA TECHNICAL REPORT ERL 228-AOML 7-2

Sea Surface Topography From Space
Volume II

Proceedings of a Conference Sponsored Jointly by
The National Oceanic and Atmospheric Administration,
The National Aeronautics and Space Administration,
and The United States Navy, Key Biscayne, Florida
October 6-8, 1971

Host Organization: Atlantic Oceanographic and Meteorological Laboratories, Environmental Research Laboratories, National Oceanic and Atmospheric Administration, U.S. Department of Commerce

JOHN R. APEL, Editor

BOULDER, COLO.
May 1972

For sale by the Superintendent of Documents, U. S. Government Printing Office, Washington, D. C. 20402
Price $1.25

THE ENERGY BALANCE OF WIND WAVES AND THE REMOTE SENSING PROBLEM

K. Hasselmann*

Institute of Geophysics
University of Hamburg

ABSTRACT

Measurements of wave growth during the Joint North Sea Wave Project (JONSWAP) indicate an energy balance of the wave spectrum governed primarily by input from the atmosphere, nonlinear transfer to shorter and longer waves, and advection. The pronounced spectral peak and sharp low frequency cut-off characteristic of fetch-limited spectra are explained as a self-stabilizing feature of the nonlinear wave-wave interactions. The momentum transferred from the atmosphere to the wind waves accounts for a large part of the wind drag. Phillips' 'constant' is found to vary appreciably with fetch and wind speed, the ω^{-5} range of the spectrum representing (for intermediate frequencies not too far from the peak) an equilibrium between atmospheric input and nonlinear transfer rather than a saturation spectrum governed by wave breaking. These findings are relevant for remote microwave sensing of the sea surface by backscatter

---

*Presently at Woods Hole Oceanographic Institution
Woods Hole, Massachusetts 02543
W.H.O.I. Contribution No. 2843

and passive radiometry methods. To first order time averaged microwave signals contain information only on the short-wave region of the surface-wave spectrum, and can be related to the energy-containing long-wave part of the spectrum (the "wind-sea spectrum") only if the dynamical interrelationships between the two wavenumber ranges are properly understood. Signal signatures directly dependent on the wind-sea spectrum can be derived from higher-order backscatter (or emissivity) models, but these also are governed by the hydrodynamical coupling between short and long waves. Delay-time measurements appear to be more closely connected to significant sea-state characteristics. If the illuminated area is large compared with the characteristic wavelength of the surface (the usual case for satellite altimeters), the mean shape of the backscattered radar pulse can be related to the mean square wave height, and further sea state parameters can probably be inferred from a more detailed analysis of the pulse statistics. Interactions between short and long waves are also important in radar altimetery in producing higher-order modifications of the pulse shape which could introduce systematic errors in the measurement of mean sea level. Although JONSWAP demonstrated the significance of wave-wave interactions for the overall energy balance of the wind-sea spectrum, many

details of the spectral equilibrium in the range of high wavenumbers responsible for microwave backscattering still remain to be clarified before microwave techniques can become a reliable tool for the measurement of sea state or the determination of mean sea level to the decimeter accuracies needed for oceanographic applications.

1. INTRODUCTION

Miles' (1957) and Phillips' (1957) important work on wind-wave generation marked the beginning of a fruitful period of theoretical research in ocean wave dynamics. A number of alternative mechanisms of wave growth have since been proposed (e.g. [14] [15] [19] [21] [22] [28] [29] [44] [50]), many of which take more detailed account of the turbulent response characteristics of the atmospheric boundary layer than these first theories. Further theoretical investigations have been concerned with the effects of wave-wave scattering ([20a,b,c] [42] [54] [56]), interactions of waves with currents ([26] [31] [32] [33]), the coupling between short waves and long waves ([24] [29] [43]), white capping ([29] [4]), and other processes. A general summary of most of this work can be found in Phillips' (1966) comprehensive monograph; a more specialised presentation from the viewpoint of weak interaction theory is given in Hasselmann (1968).

Despite these continuing theoretical efforts, however, it is only very recently that field experiments have succeeded in identifying some of the principal features of the overall energy balance of the wave spectrum. Earlier field studies by Snyder and Cox (1966) and Barnett and Wilkerson (1967) revealed that Phillips' and Miles' mechanisms were too weak by almost an order of magnitude to explain the observed wave growth rates. On the basis of a series of wave growth measurements in Hakata Bay and a wind-wave tank, Mitsuyasu ([36a,b] [37] [38]) concluded later that the evolution of the spectrum was strongly influenced by wave-wave interactions as well as the energy transferred from the wind. Extensive large-scale measurements of spectral growth during the Joint North Sea Wave Project (JONSWAP, [5]) have recently confirmed Mitsuyasu's interpretation quantitatively; the characteristic, sharply peaked form of developing wave spectra and the associated rapid growth rates on the forward face of the spectrum could be explained as a self-stabilizing feature of the nonlinear wave interactions. Indirectly, the measurements also yielded an estimate of the energy and momentum transferred from the wind to the waves. The discussion of the energy balance of wind-wave spectra in the first part of this review will accordingly be based primarily on the picture that has evolved from the analysis of the JONSWAP data.

The question of the surface-wave energy balance turns out to be closely related to the problem of remote sea-surface sensing, which is considered in the second part of this paper. One of the goals of remote measurements from satellites is to obtain synoptic data of sea state and, if possible, surface winds as input for wave and weather forecasts. The quality of data needed for this purpose is determined by the numerical prediction model used, which in the case of surface waves is governed by the structure of the spectral energy balance. More importantly, the interpretation of microwave signals emitted or scattered from the sea surface is intimately dependent on the details of the dynamical interactions affecting the energy balance of the wave spectrum. This applies both to measurements of the sea state itself as also to the determination of the wave-induced noise in measurements of other properties of the sea surface, such as the microwave temperature or the mean surface elevation.

The relevance of dynamical processes for the — apparent purely kinematical — problem of determining sea state results from a basic difficulty besetting microwave measurements: the pronounced wavelength mismatch between the sensing radiation and the wave field being sensed. This precludes determining the surface wave spectrum directly by

standard linear scattering methods. To lowest order the backscattered signals (for finite angles of incidence) yield information only on the cm-dm wavelength components of the spectrum. The "wind-sea spectrum" itself (using the term here to denote the wavelength region of the spectrum between about 5 m and 500 m which contains most of the surface wave energy) is accessible to measurement only indirectly through higher order signal characteristics arising from hydrodynamic and electromagnetic interactions between the short scattering waves and longer waves.

We are still far from a complete understanding of the many processes contributing to this coupling. The JONSWAP results indicate that most of the energy received by the short waves is transferred across the spectrum from the longer waves, rather than directly from the atmosphere. Unfortunately, the measurements did not extend to the very short waves in the cm-dm range responsible for microwave scattering. Moreover, this range of the spectrum poses theoretical difficulties in that the coupling of very short waves to the wind-sea spectrum cannot be treated by the resonant interaction theory applicable within the wind-sea spectrum itself (cf. [24]). In particular, it appears that, in contrast to resonant interactions, a consistent treatment of short-long wave interactions must include dissipation and the coupling with the wind. To achieve quantitative microwave measurements of sea state, surface winds, or other sea-

surface properties affected by wave noise, detailed experiments will be needed to extend the picture of the spectral energy balance derived from JONSWAP to the higher wavenumbers in the Bragg scattering range.

2. THE RADIATIVE TRANSFER EQUATION

It is known that to a good approximation wind-generated ocean waves obey the linearized hydrodynamic wave equations for irrotational flow. Linearity implies that the wave field is closely Gaussian [21] and can be fully characterized by its two-dimensional energy spectrum $F(\underset{\sim}{k})$ with respect to horizontal wavenumber $\underset{\sim}{k}$, where

$$\iint_{-\infty}^{\infty} F(k)\, d\underset{\sim}{k} = \text{mean square wave height } \langle \zeta^2 \rangle$$

$$(= \text{wave energy/g.})$$

Experimentally, wave spectra are usually determined through frequency analysis of surface displacements measured at a fixed position, and it is therefore convenient to introduce also the two dimensional spectrum $E_2(f,\theta)$ with respect to frequency $f = \omega/2\pi$ and propagation direction θ, $E_2(f,\theta)\, df d\theta = F(\underset{\sim}{k})\, d\underset{\sim}{k}$. The transformation Jakobian follows from the (deep-water) dispersion relation $\omega = (gk)^{\frac{1}{2}}$: $df d\theta = 2\pi k v^{-1}\, d\underset{\sim}{k}$, where $v = \frac{1}{2}(g/k)^{\frac{1}{2}}$ is the modulus of the group velocity $v_\alpha = \partial\omega/\partial k_\alpha$ $(\alpha = 1,2)$. Integration over the propaga-

tion directions yields the one-dimensional frequency spectrum $E(f) = \int_{-\pi}^{\pi} E_2(f,\theta)\,d\theta$

Since each "wave packet" of the spectrum propagates with a group velocity appropriate to its wavenumber $\underset{\sim}{k}$, densities at different times t and positions $\underset{\sim}{x}$ in the ocean are interrelated through the spectral energy balance or radiative transfer equation (neglecting refractive effects)

$$\frac{dF}{dt}(\underset{\sim}{k};\underset{\sim}{x},t) \equiv \frac{F}{t} + \underset{\sim}{v}\cdot\Delta F = S \quad . \tag{1}$$

The left-hand side of the equation expresses the conservation of spectral energy density along the path of a wave group, in accordance with the conservation of energy of individual wave packets as given by the linear, free-wave theory, while the right hand side S represents the net change in energy of the component $\underset{\sim}{k}$ due to all dynamical processes not included in the linear theory. The source function can be represented generally as a superposition

$$S = S_{in} + S_{tr} + S_{ds}$$

of the input S_{in} due to air-sea interactions, a transfer term S_{tr} representing a redistribution of energy within the spectrum conserving total wave energy and momentum, and a dissipation term S_{ds}.

Once the dependence of S on the wave spectrum and

the local wind has been established, the problem of wave prediction for a given wind field reduces to the numerical integration of the radiative transfer equation under appropriate initial and boundary conditions for the wave field. Until recently, however, forecasting methods based on this approach ([2] [3] [18] [45] [47]) have been severely handicapped by lack of quantitative measurements of the wave energy balance, which have made it difficult to decide between a number of strongly differing proposed source-function models, cf [22].

3. THE JOINT NORTH SEA WAVE PROJECT

One of the purposes of JONSWAP was to obtain information about the source function suitable for the needs of practical wave forecasting. A second goal was to gain insight into the relative significance of the various interaction processes contributing to the overall energy balance of the wave field.

To determine rates of change of the wave spectrum, simultaneous wave measurements were made at 13 stations along a 160 km profile extending westward from the island of Sylt in North Germany (Figs. 1 and 2). Half-hourly recordings were made six to twelve times daily for a period of 10 weeks in July-August of 1969; additionally, 4 weeks of data were obtained in September 1968 during a pilot experiment with a

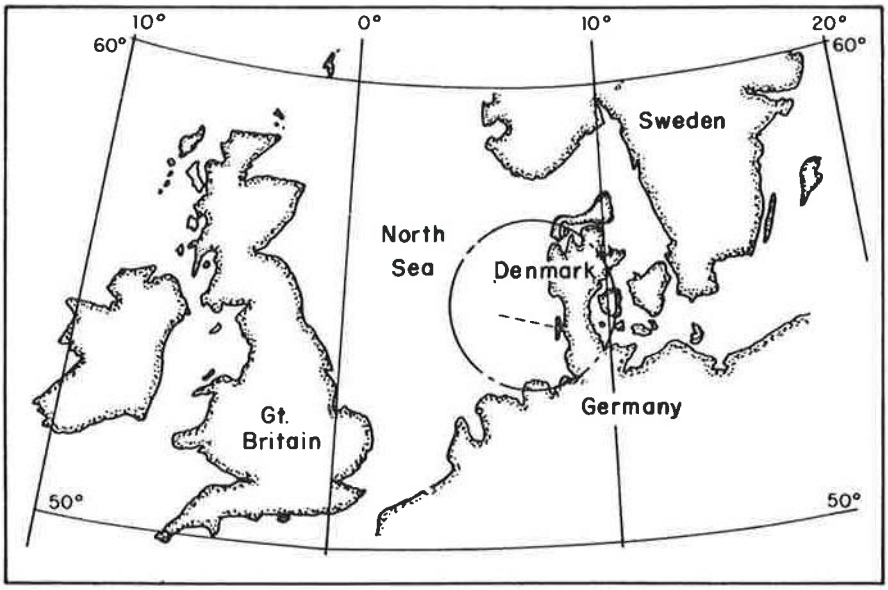

Figure 1. Site of Joint North Sea Wave Project.

STATION	INSTRUMENT	INSTITUTE
1, 2, 3, 5,	WAVE POST	DHI, HAMBURG
4	6 INSTRUMENT WAVE ARRAY	WESTINGHOUSE, SAN DIEGO
7, 9, 10	WAVE RIDER	KMNI, DE BILT
6, 10, 11 12, 13	PITCH AND ROLL BUOY	DHI, HAMBURG NIO, WORMLEY
8	HOT WIRE, CUP AND VANE ANEMOMETERS WAVE POST	GI, HAMBURG DHI, HAMBURG

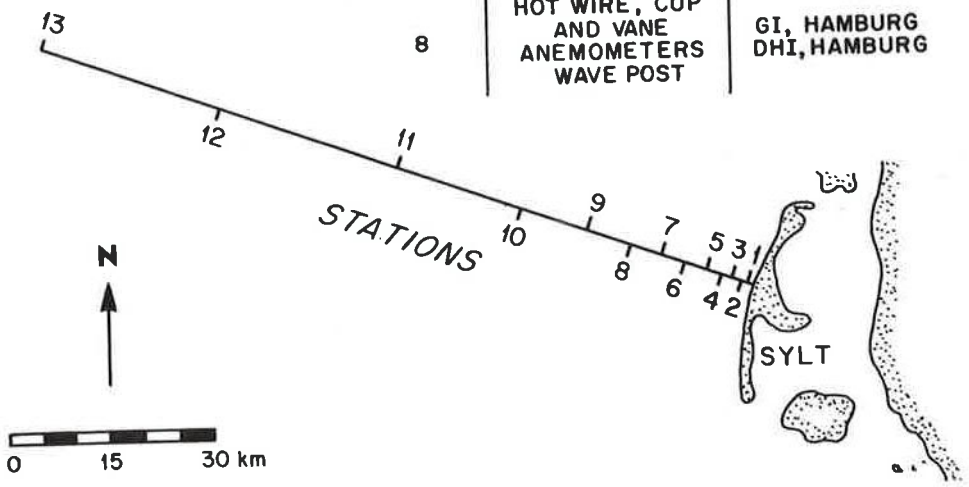

Figure 2. The JONSWAP profile.

reduced profile. A variety of wave recorders, about half of which yielded directional resolution as well as wave heights, were deployed (cf. table, Fig. 2). Extensive measurements were made also of winds, currents, temperatures and other environmental parameters (for a summary of the objectives and logistics of the experiment, cf. Barnett (1970)).

Optimal conditions for studying wave growth obtained when the wind was blowing offshore in a direction parallel to the profile. In this case, cross-profile variations of the wave field were small, and the source function could be evaluated by differentiating the observed spectra with respect to time and the spatial coordinate parallel to the profile.

Figure 3 shows a typical series of one-dimensional spectra measured under these conditions. To summarize the observed growth behavior, the spectra were parametrized by best-fitting an analytic function containing five free parameters. The frequency scale of the fitting function was defined by the frequency f_m at the spectral peak, the ordinate scale α by adjusting a Phillips (1958, 1966) saturation spectrum $\alpha g^2 (2\pi)^{-4} f^{-5}$ to the high-frequency part of the observed spectrum. The remaining three shape parameters $\sigma_a, \sigma_b, \gamma$ characterized the form of the narrow peak in the transition zone between zero energy at low frequencies and the high-frequency f^{-5} regime.

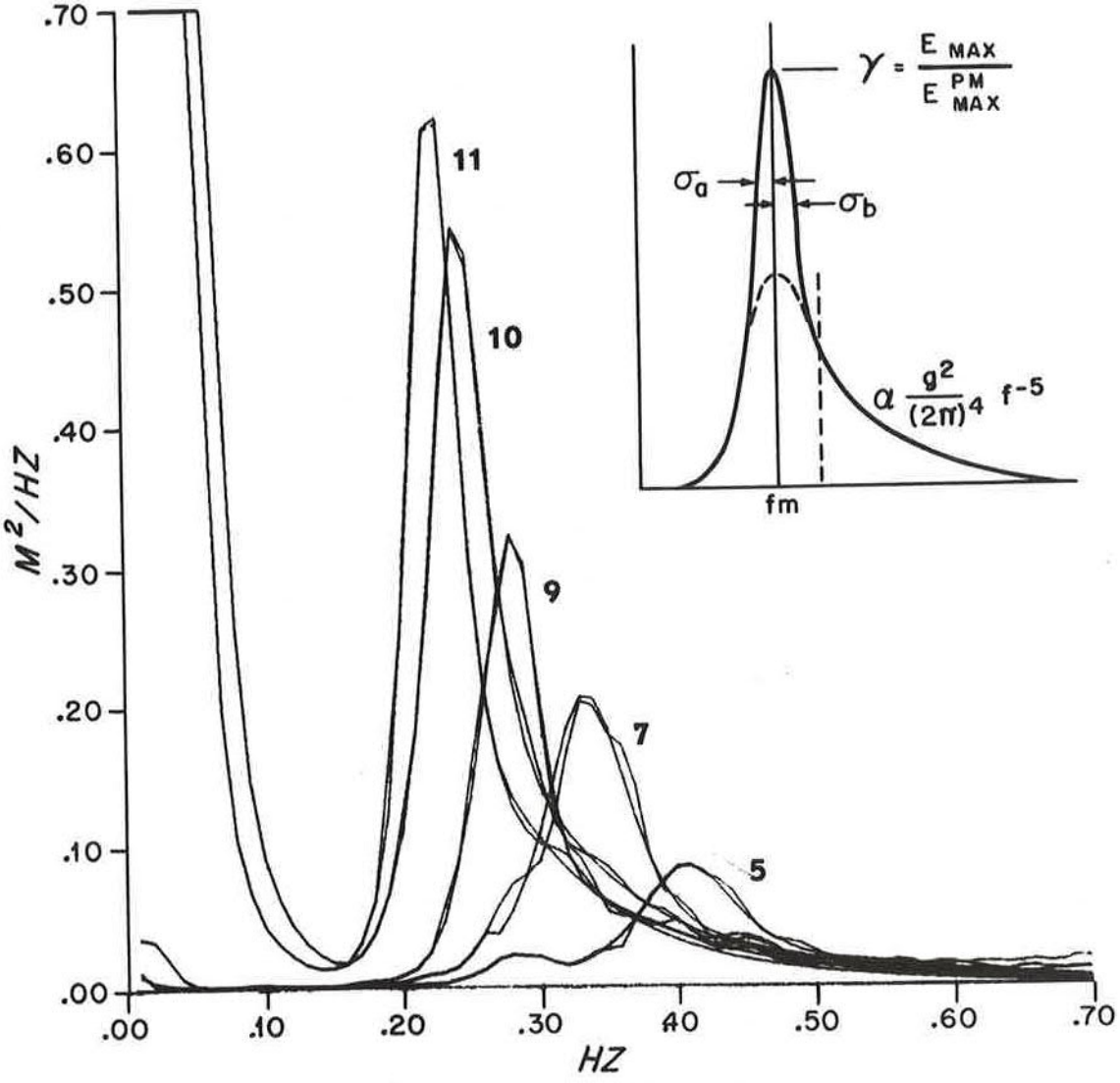

Figure 3. Growth of wave spectra for offshore (east) wind conditions. Fetch increases from Station 5 through Station 9. Best-fit analytic shapes are superimposed on the observed spectra; the five free parameters f_m, α, δ_a, δ_b and $\gamma = E_{max}/E^{P-M}_{max}$ (PM ≡ Pierson-Moskowitz) of the fitting function are indicated in the inset.

In most of the generation cases studied, the time derivative in the energy balance equation was small compared with the convective term. By dimensional arguments, Kitaigorodskii (1962) has shown that the nondimensional wave spectrum $\hat{E}(fu_*/g) = g^{-3}u_*^5 E(f)$ should reduce in this case to a universal function of the nondimensional fetch $\hat{x}$ = (fetch) $\cdot g/u_*^2$, where the friction velocity u_* = (momentum τ transferred across the air-sea interface/density of air)$^{\frac{1}{2}}$. The dependence of the scale parameters on $\hat{x}$ is shown in Fig. 4. Note that α decreases with $\hat{x}$, in contrast to Phillips' original dimensional argument, which predicts a universally constant α. This is in accordance with the interpretation of the source function given below which indicates that the f^{-5} dependence in this part of the spectrum is not dominated by white capping, as assumed by Phillips, but rather by a balance between the energy input from the atmosphere and the energy transfer to other wave components through wave-wave interactions.

The shape parameters showed considerable scatter, but no systematic variation with fetch [5]. Within the uncertainties of this variability (attributed to the gustiness of the wind), the wave spectra could be regarded as self similar over the range of fetches of the experiment.

The smoothed dependence of the five spectral parameters on nondimensional fetch $\hat{x}$ defined a mean evolution of

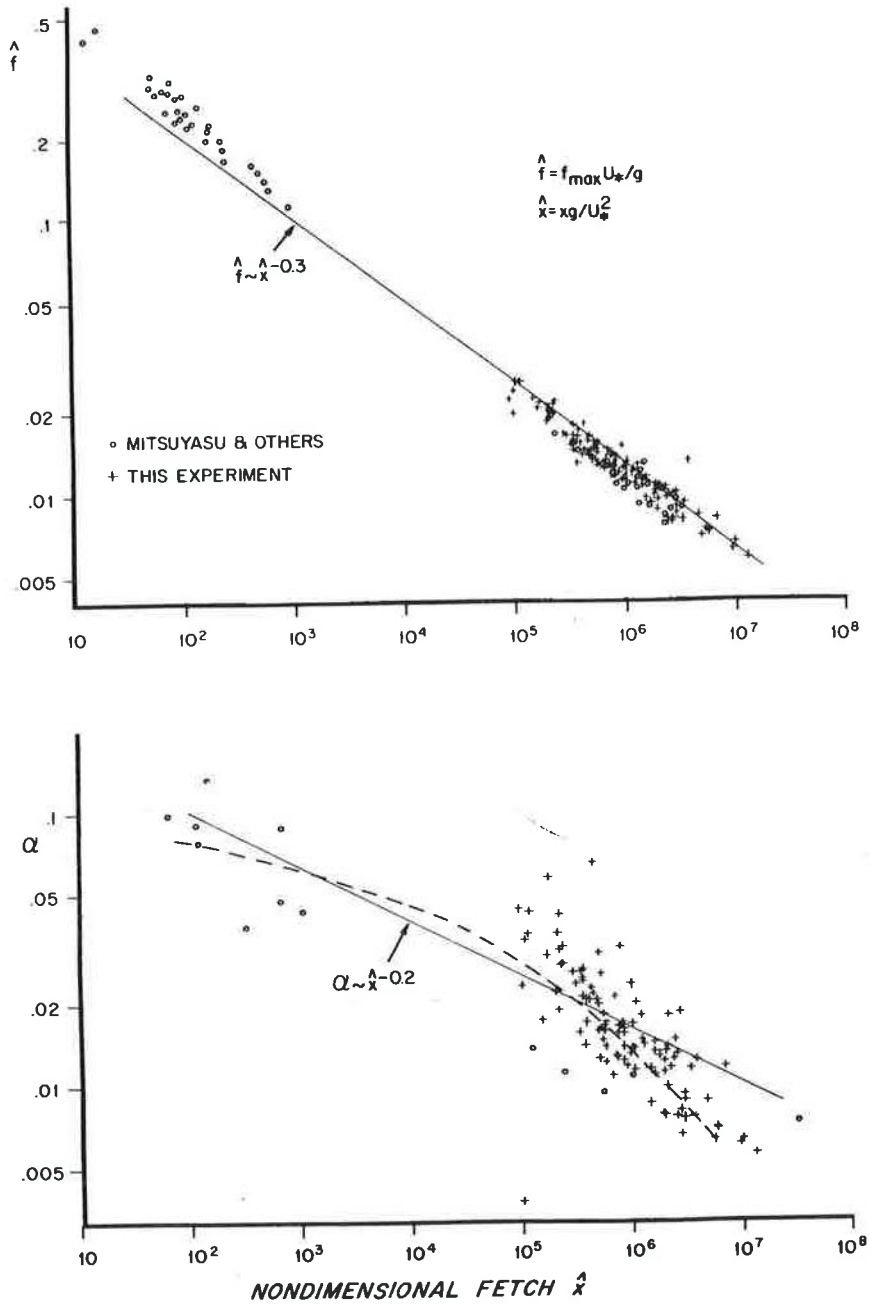

Figure 4. Variation of scale parameters with nondimensional fetch. The friction velocity is taken as $u_* = (1.2.10^{-3})^{\frac{1}{2}} U_{10}$. ($U_{10}$ = wind speed at 10 m height above the mean surface.)

of the spectrum, from which a mean source function was then determined through the energy balance equation (1). The characteristic +- distribution of the source function (cf. Fig. 5) is due to the shift of the spectral peak towards lower frequencies. The positive lobe corresponds to the rapid wave growth on the forward face of the spectrum; after the peak has passed to lower frequencies, the components on the right of the peak then decay again before approaching a quasi-stationary equilibrium value (cf. also Fig. 3).

4. THE ENERGY TRANSFER DUE TO WAVE-WAVE INTERACTIONS

This "overshoot" phenomenon has been observed independently by several workers in field and laboratory experiments ([6] [7] [36a,b] [37] [53]). Barnett and Sutherland (1968) suggested nonlinear wave-wave interactions as a possible explanation, a conjecture which later found some support by Mitsuyasu's (1968) estimates of the nonlinear transfer rates for a decaying spectrum in a wave tank. The calculations were based on Barnett's (1968) parametrization of the Boltzmann scattering integrals computed in Hasselmann [20c]. Exact computations of the nonlinear transfer integrals for a number of JONSWAP spectra ([5] [50]) have confirmed that the principal features of the observed source function can indeed be explained by resonant wave-wave interactions: Fig. 5 shows that both the overshoot and the

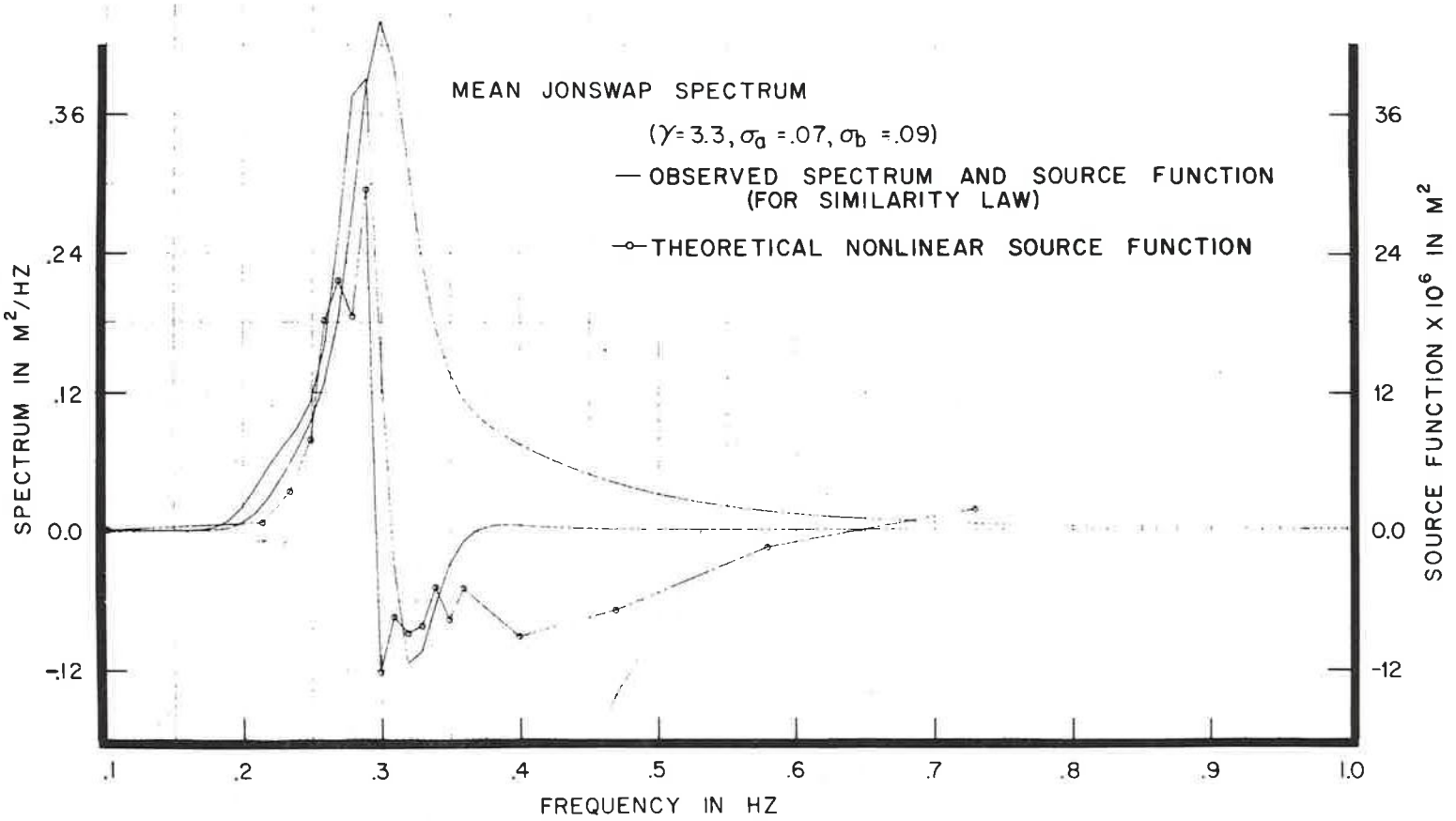

Figure 5. Mean JONSWAP spectrum, empirical mean source function, and the nonlinear energy transfer as computed from the mean JONSWAP spectrum. A $\cos^2\theta$ spreading function was assumed. The curves shown here for a particular windspeed and fetch remain valid for all windspeeds and fetches if the axes are scaled appropriately.

major part of the rapid growth on the forward face of the spectrum can be attributed to the nonlinear transfer.

The basic mechanism of the process is illustrated in Fig. 6. According to the classical theory of lowest order Bragg scattering, an incident wave i can be refracted by a sinusoidal disturbance c (e.g., one of the harmonics of a periodic lattice, or a second wave component) into a scattered wave s, provided some form of nonlinear coupling exists between c and the incident and scattered waves, and the three components satisfy the Bragg relations for constructive interference (resonance)

$$\sigma_i \omega_i + \sigma_c \omega_c = \omega_s$$
$$\sigma_i k_i + \sigma_c k_c = k_s \quad (\sigma_i \sigma_c = \pm) \qquad (2)$$

It can be shown that these conditions cannot be satisfied by three gravity wave components — or in general by any three waves having the same dispersion relation for which the curvature $d^2\omega/dk^2$ is negative throughout. However, Bragg scattering can occur at second order. On account of weak nonlinear interactions, the spectrum of surface displacement continues not only free-wave components ($\omega, \underset{\sim}{k}$) but also all combinations of quadratic harmonics ($\omega_1 \pm \omega_2, \underset{\sim}{k}_1 \pm \underset{\sim}{k}_2$) generated by pairs of free waves ($\omega_1, \underset{\sim}{k}_1$), ($\omega_2, \underset{\sim}{k}_2$) (plus cubic and higher order harmonics of correspondingly smaller amplitude).

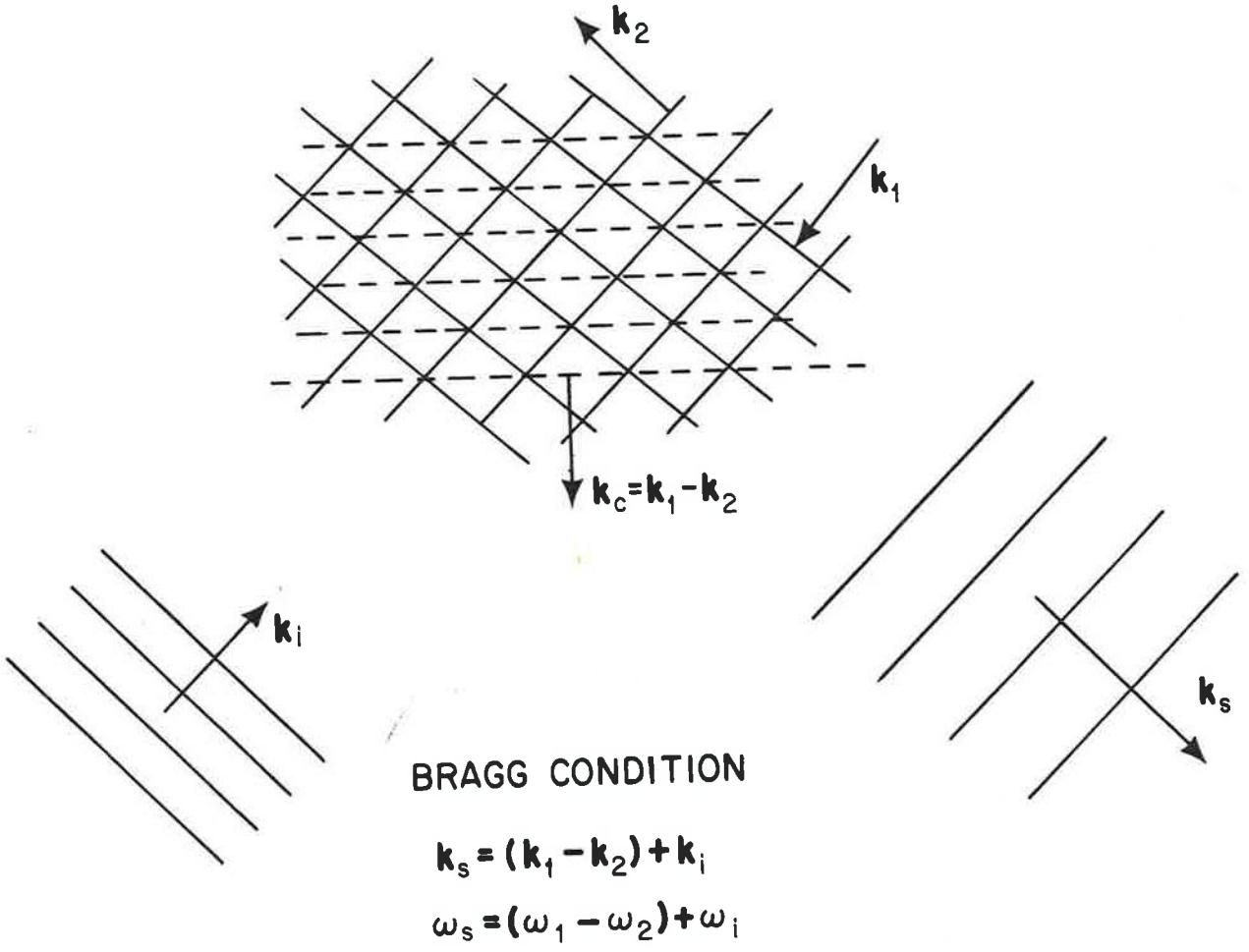

Figure 6. Second-order Bragg scattering (cubic wave-wave interactions).

These forced, non-propagating components can act as the component **c** in Fig. 6 coupling the free incident wave **i** to the scattered free wave **s** . For the lowest order interaction with a quadratic harmonic, the Bragg condition is accordingly given by ([20a] [42])

$$\sigma_i \omega_i + \sigma_1 \omega_1 + \sigma_2 \omega_2 = \omega_s$$

$$\sigma_i \underset{\sim}{k}_i + \sigma_1 \underset{\sim}{k}_1 + \sigma_2 \underset{\sim}{k}_2 = \underset{\sim}{k}_s$$

The net coupling is cubic in the wave amplitudes, the scattered wave **s** being generated by a quadratic interaction between the free incident wave **i** and the forced wave **c** , which itself is produced by a quadratic interaction between two free waves 1 and 2. For a continuous spectrum, the summation over all possible interactions of this kind yields an energy transfer rate given by a Boltzmann integral over combinations of cubic products of the spectral densities at the four wavenumbers occurring in each scattering process ([20a]). The structure of the integral is rather complex, and it has not been possible to find a simple explanation for the particular form of the nonlinear transfer rates computed for the different cases shown, for example, in Figs. 5 and 7. The H theorem, which states generally that wave-wave scattering changes the spectrum irreversibly in the direction towards a uniform

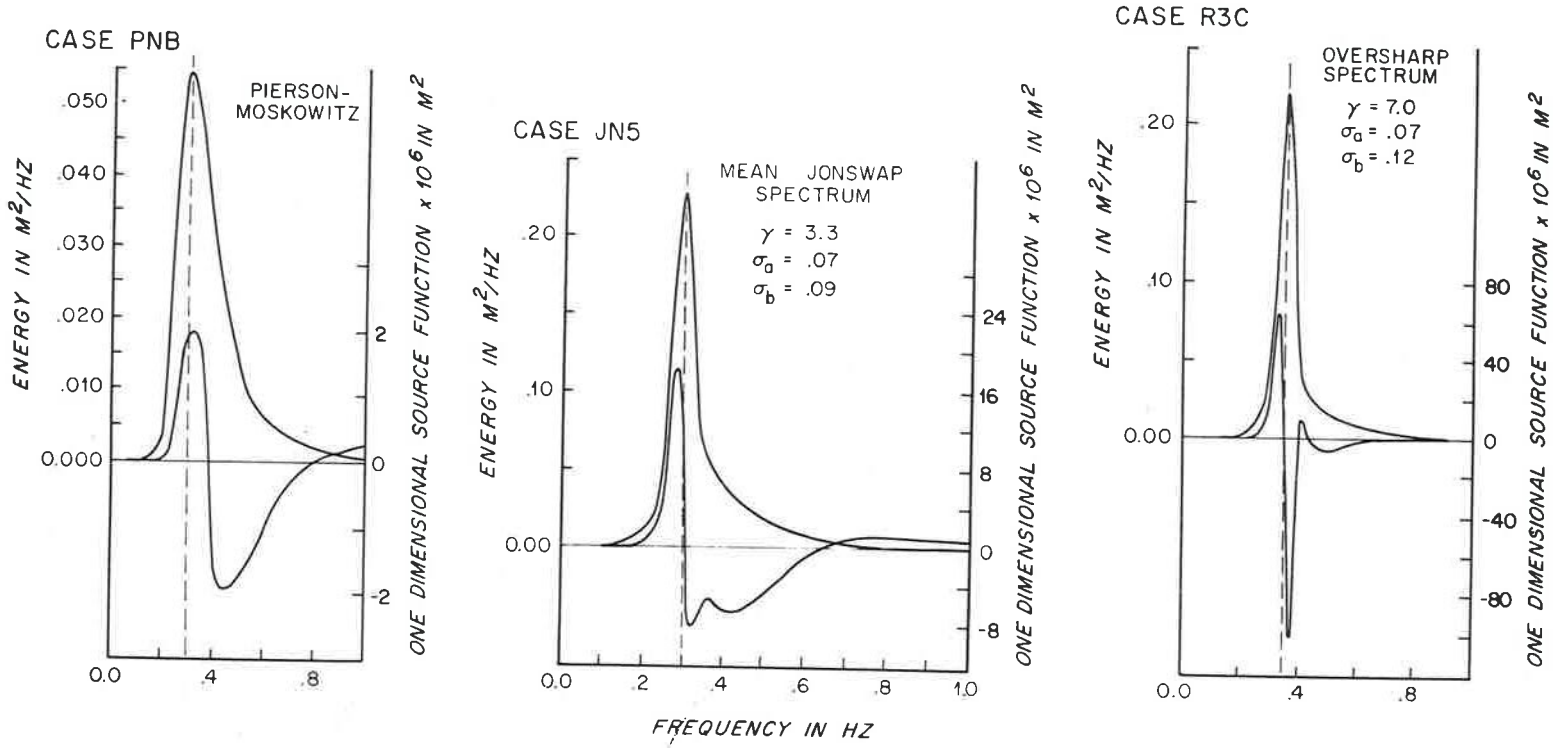

Figure 7. Nonlinear transfer rates computed for three differently peaked spectra. The flatter peak on the left (corresponding to a Pierson-Moskowitz spectrum) is growing, whereas the sharper peak on the right is broadening and shifting towards lower frequencies. The mean JONSWAP spectrum in the center corresponds to the stable case in which the peak shifts without appreciable change in shape. Computations are based on $\cos^2\theta$ spreading factors.

energy distribution in wavenumber space, in conjunction with the constraints of momentum, energy and — in this case — action conservation, explain the general +-+ distribution of the nonlinear source function [20b], but not the positions of the individual lobes, which turn out to be essential for the stability of the spectral shape.

5. THE OVERALL ENERGY BALANCE

It follows from the computed nonlinear transfer rate shown in Fig. 5 that for a spectrum of the general JONSWAP form wave-wave interactions will produce a shift of the peak towards lower frequencies at about the rate observed. However, this says nothing about the origin of the peak, or its persistence once it has been generated. To resolve these questions, computations of the nonlinear energy transfer were made for a series of spectral shapes which were either broader or more sharply peaked than the mean JONSWAP spectrum. It was found that the peak appears to be a self-sustaining feature of the nonlinear energy transfer which evolves from almost any initial spectral distribution, independent of the details of the energy input.

As an example, the left panel in Fig. 7 shows the nonlinear transfer for a spectrum with a less pronounced peak than the mean JONSWAP spectrum. Characteristic for these broader distributions (in this case a Pierson-Moskowitz spectrum) is the position of the positive lobe

of the nonlinear source function directly beneath the spectral maximum, causing the peak to grow. As the peak develops, the positive lobe moves towards the forward face of the spectrum until a stage is reached, corresponding roughly to the mean JONSWAP spectrum, where the peak no longer grows but merely shifts towards lower frequencies without appreciable change in shape (2nd panel). For a still sharper peak, shown in the third example, the source function develops two positive lobes immediately adjacent to a strong negative lobe beneath the spectral maximum, and the peak broadens again.

The evolution of this self-stabilizing spectral shape does not appear to be affected qualitatively by the details of the energy input from the atmosphere or the dissipation; these determine the energy level of the spectrum and the rate at which the nonlinear transfer causes the peak to wander towards lower frequencies, but not the basic form of the energy distribution resulting from the combination of the three source terms.

The probable decomposition of the net source function S into its three constituents S_{in}, S_{tr} and S_{ds} is shown in Fig. 8. Of the four terms in the equation

$$S = S_{in} + S_{tr} + S_{ds}$$

only the terms S (measured) and S_{tr} (computed)

were determined quantitatively. These define also the sum $S_{in} + S_{ds}$, but the further separation into the individual contributions S_{in} and S_{ds} shown in Fig. 8 is somewhat speculative. Fortunately, the ambiguity is somewhat restricted in this case by the side condition that the total momentum transferred from the atmosphere to the wave field cannot exceed the total momentum transferred across the air-sea interface, which is reasonably well known from flux measurements in the atmospheric boundary layer (also made during JONSWAP). Assuming negligible energy dissipation in the main part of the spectrum, as in Fig. 8, the net transfer of momentum from the atmosphere to the wave field is found to account for 50% ±30% of the total momentum lost from the atmosphere. (Since the ratio of momentum to energy for each wave component is equal to $\underset{\sim}{k}/\omega$, the spectral momentum transfer to the waves is given by $S_{in} \cdot \underset{\sim}{k}/\omega \cdot A \cos^2\theta$ angular distribution was assumed in carrying out the integration.) Dobson (1971) and Synder (personal communication) also found that a major part of the momentum lost by the atmosphere enters the wave field. If dissipation is added to the energy balance, the atmospheric input has to be increased accordingly in order for the sum $S_{in} + S_{ds}$ to remain constant. Clearly, a very large dissipation is not acceptable within the limitations set by the total transfer across the air-sea interface.

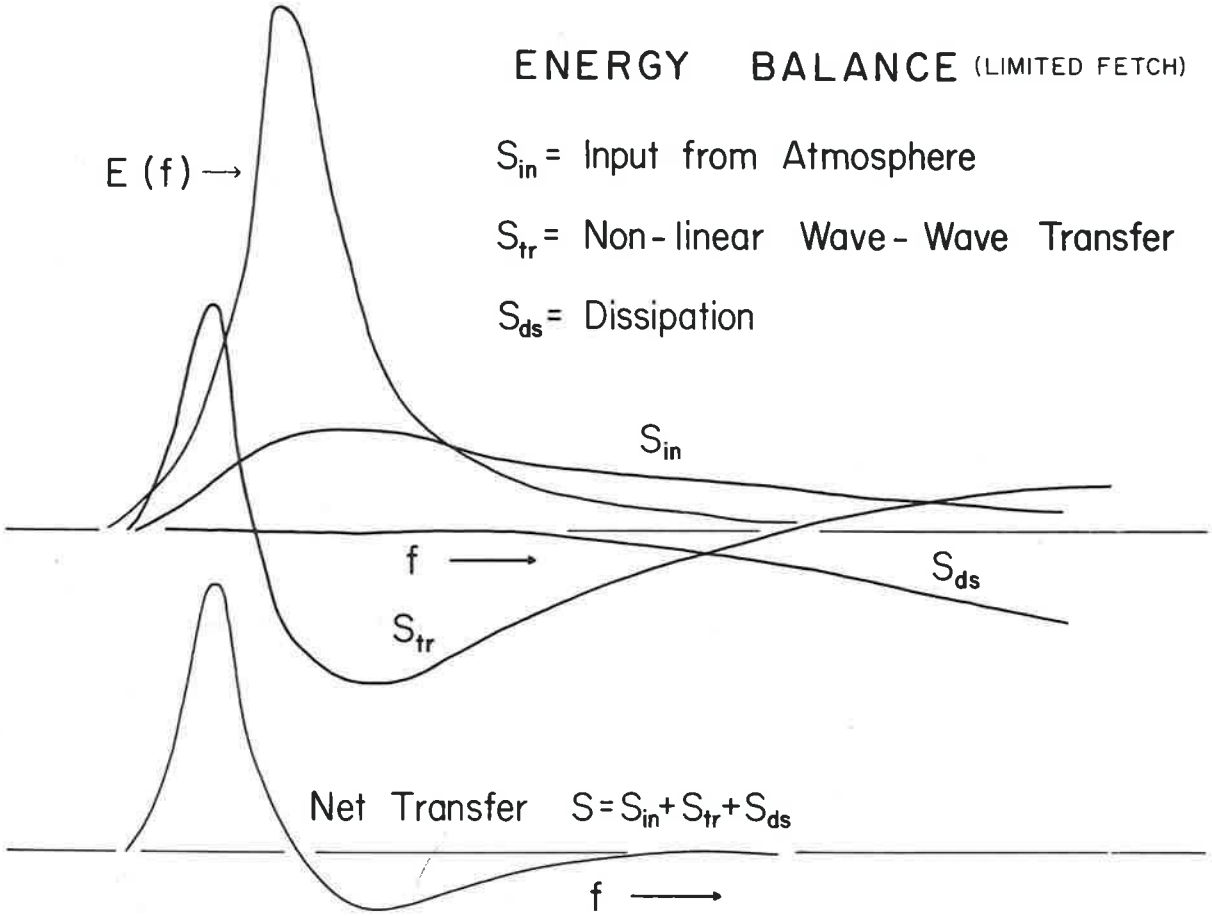

Figure 8. Decomposition of the measured total source function $S = S_{in} + S_{tr} + S_{ds}$ into its individual constituents. S, S_{tr} and $(S_{in} + S_{ds})$ can be either measured or computed, but the separation of $S_{in} + S_{ds}$ into components is tentative (see text).

According to this picture, the development of the wave spectrum for finite fetches is governed primarily by the energy balance between the atmospher input S_{in} and the nonlinear transfer of energy S_{tr} from the main part of the spectrum to lower and higher frequencies. Under stationary conditions the low-frequency energy generated by wave-wave interactions is convected away, $\underset{\sim}{V}\cdot\nabla F \approx S_{tr}$, whereas at high frequencies the energy gain due to the nonlinear transfer and the atmospheric input has to be balanced by some dissipative mechanism. About 10% of the total momentum transferred across the air-sea interface is convected away by the low-frequency waves. This can be deduced from the increase of the total momentum of the wave field with fetch, independent of the source function analysis. Between 15 and 60% of τ is accounted for by the nonlinear transfer* of momentum from the main part of the spectrum to shorter waves ($f > 0.7$ Hz in Fig. 5), where it is converted to current momentum by dissipation. Again, this estimate is independent of details of the energy balance, following alone from the nonlinear transfer rates computed for the observed spectra. To balance these momentum fluxes, about 50% ±30% of the momentum transferred across the air-sea interface must be entering the wave field in the central region of the spectrum.

* The uncertainty reflects the sensitive dependence of these computations on the spectrum.

Several questions remain unanswered in this description. Although the inferred momentum transfer rate from the atmosphere to the wave field can be shown to scale in accordance with a linear process [5], as predicted by the majority of wave-generation theories, and yields a drag coefficient independent of wind and fetch, as generally observed, the actual mechanism of wave generation by wind has not been determined. The existence of an asymptotic, fully developed spectrum at very large fetches is another open point. Without some mechanism for extracting energy from very long waves, the nonlinear transfer would continue to generate longer and longer waves indefinitely. Possible candidates for a long-wave energy sink are the attenuation by the wind of waves traveling at phase speeds exceeding the wind speed, which has found some support in recent laboratory experiments [51], or the transfer of energy from long waves to very short waves (which lie beyond the range of resonant-interaction theory) via WKBJ interactions [24]. The latter process is also relevant for a third unresolved problem, the form of the energy balance at high wavenumbers. Since 70% ±20% of the momentum flux to the waves is transferred to short waves via the long waves and wave-wave interactions, a significant energy and momentum sink is needed at high wavenumbers. Valenzuela (1971) has shown

that for very short waves energy can be rapidly transferred to higher wavenumbers through gravity-capillary interactions, which satisfy the Bragg resonance conditions already at second order (cf. Phillips, 1966). In this case, the energy sink could be viscosity acting on extremely short waves. Estimates indicate that this could remove all the energy supplied to the wave field for wind speeds up to a few m/s, but at higher winds energy is presumably lost over a broader band of wavenumbers through white capping. The resolution of these questions is fundamental for the application of microwave techniques, which sense primarily the very short surface waves and are therefore critically dependent on the ability to predict the energy level in this wavenumber range as a function of the wind-sea spectrum and the local wind speed.

6. STATISTICAL DESCRIPTION OF BACKSCATTER

In order to discuss further the implications of wave dynamics for the remote sensing problem, we first review briefly the concepts and models developed to interpret microwave measurements of the sea surface. It is found that these models lead naturally to the same questions that arose in the consideration of the wave energy balance. For simplicity, we restrict the discussion to active microwave techniques. Microwave temperature measurements are also

strongly influenced by the wave field, but the passive emission problem is rather analagous to the scattering case in the sense that similar interaction models are applicable in both instances.

Space measurements of sea surface backscatter are best made in the cm-dm wavelength band in order to combine good beam resolution with weak transmission losses in the atmosphere. Synoptic coverage of the sea surface over distances extending to several thousand kilometers can also be achieved with land stations using decameter waves reflected from the ionosphere. It has been shown that at these wavelengths the higher-order doppler side bands of the sea echo can be related theoretically to the one-dimensional frequency spectrum of the wave field ([23] [25] [8]). The interactions in this case involve relatively long wind waves and are reasonably well understood. However, we restrict ourselves here to microwave techniques applicable to satellites; unfortunately, these are governed by interactions in the less studied and dynamically more complicated high wavenumber region of the surface wave spectrum.

The backscattered return from pulsed microwave emission contains statistical amplitude, phase and travel time information, which can be largely summarized in terms of the second moments of the signal. In the particular case that the process is Gaussian, these provide a complete statisti-

cal description of the backscattered return. According to the Central Limit Theorem, this will approximately apply (independent of the sea-surface statistics) if the footprint diameter is large compared with the correlation scale of the scatterers — a condition which is often satisfied in satellite applications. However, an interesting technique exploiting non-Gaussian properties of backscattered modulated microwaves [48] is mentioned in §8. In this case the non-Gaussian signature, although small, can be readily filtered out of the much larger Gaussian components. Useful sea-state information can also be obtained from the initial return characteristics of altimeter pulses, which correspond to the non-Gaussian, small footprint limit (§9). The non-Gaussian properties of these signals have not been systematically investigated, but a preliminary inspection indicates that they are related to useful wavelength distributions of the wind-sea not contained in the second moments of the signal.

A backscattered microwave pulse centered at the frequency ω_o may be expressed in the form

$$V(t;\tau) = B(t;\tau)e^{i\omega_o t}$$

where $B(t;\tau)$ is a random complex modulation factor (complex envelope) depending on the delay time t relative to the time of emission τ of the pulse. For fixed τ, $B(t)$ defines the shape of the backscattered pulse, the

(much slower) variation of pulse shape with τ arising then through the time dependence of the backscattering surface. Assuming that the scattering process is statistically stationary with respect to τ and that the phase distribution of B is statistically uniform, the first moment of B vanishes and the second moments are given by

$$\langle B(t_1, \tau'+\tau)\, B^*(t_2,\tau')\rangle = R(t_1,t_2,\tau)$$

$$\langle B(t_1, \tau'+\tau)\, B(t_2,\tau')\rangle = 0$$

The ensemble averages $\langle \cdot\cdot\cdot \rangle$ may be interpreted here also as time means with respect to τ'.

The doppler spectrum of the general second moment is defined as the Fourier transform

$$T(t_1, t_2, \omega) = \frac{1}{2\pi}\int_{-\infty}^{\infty} R(t_1, t_1, \tau)e^{-i\omega\tau}d\tau.$$

T depends on both the shape of the emitted pulse and the statistical properties of the scattering surface. The two effects may be separated by introducing the scattering function, which describes the (input independent) second-moment statistics of the time-varying "channel" representing the backscattering sea surface, cf [17].

In terms of the oomplex envelope $A(t)$ of the transmitted pulse, the received pulse can be expressed in the

general form

$$B(t, \tau) = \int_{-\infty}^{\infty} x(t', \tau) A(t-t') dt'$$

where the linear filter $x(t, \tau)$ represents the distortion of the pulse due to the backscattering surface. The second moment of the signal is therefore given by

$$R(t_1, t_2, \tau) = \iint_{-\infty}^{\infty} \langle x(t', \tau'+\tau) x^*(t'', \tau') \rangle A(t_1-t') A^*(t_2-t'') dt' dt''$$

For most scattering models (including the ones discussed here) the autocorrelation of the filter function is significantly non-zero only for time differences $t' - t''$ of the order of the carrier period. Hence in integrating over the much longer pulse duration the second moment of x may be approximated by a σ -function,

$$\langle x(t', \tau'+\tau) x^*(t'', \tau') \rangle = P(t', \tau) \delta(t'-t'')$$

which yields

$$R(t_1, t_2, \tau) = \int_{-\infty}^{\infty} A(t_1-t') A^*(t_2-t') P(t', \tau) dt'$$

or, in terms of the doppler spectra,

$$T(t_1, t_2, \omega) = \int_{-\infty}^{\infty} A(t_1-t') A^*(t_2-t') S(t', \omega) dt'$$

where

$$S(t, \omega) = \frac{1}{2\pi} \int_{-\infty}^{\infty} P(t,\tau) e^{-i\omega\tau} d\tau$$

is the scattering function.

Neither measurements nor a comprehensive theoretical analysis of the complete doppler spectrum or scattering function for a random sea surface appear to have been attempted. Published investigations have considered either the scattering cross sections i.e., the mean power of the backscattered pulse

$$\sigma = \iint T(t,t,\omega)\, dt\, d\omega$$

and its doppler decomposition

$$f(\omega) = \int T(t,t,\omega)\, dt\ ,$$

both of which average out the travel time information (and can therefore be determined from CW-type measurements), or alternatively the mean pulse power

$$I(t) = \int T(t,t,\omega)\, d\omega$$

as a function of delay time, which makes no use of the doppler information.

Cross-section and doppler measurements are normally made at finite angles of incidence, whereas travel-time data has been obtained largely from altimeters operating at near normal incidence. Different scattering models are

found to be valid in each of these ranges of incident angle, so that the following discussion of backscatter models will naturally tend to emphasize the type of measurement associated with a given model. However, it is conceivable that a more detailed investigation of the properties of the complete doppler spectrum or scattering function would reveal valuable additional sea state signatures not discernible in the usual measurements but nonetheless accessible by standard linear signal processing techniques.

7. THE SPECULAR REFLEXION AND BRAGG SCATTERING MODELS

The simplest description of surface scattering is the specular reflexion of an ensemble of rays by a statistical distribution of infinitesimal surface facets, as originally applied by Cox and Munk [12] [13] to the analysis of sun glitter from the sea surface. For microwaves, the model is applicable for angles of incidence less than about 20° from the vertical. At larger angles, specular reflexion becomes negligible and the backscatter is dominated by first-order Bragg interactions in accordance with the resonance conditions (2). These define two backscattering surface-wave components with wavelengths equal to half the horizontal wavelength of the incident radiation, propagating towards or away from the microwave source.

Both models are found to be in good accord with obser-

vations in their regions of theoretical validity (cf [9] [10] [49] [57]), but yield only limited information on the wind-sea spectrum in terms of the cross sections and doppler spectra, cf. table 1 (the application of the specular reflexion model to altimeter data is discussed in §9). The Bragg model determines only the wave spectrum at the two (very high) Bragg wavenumbers. The specular reflexion model yields the mean square wave slope and vertical orbital velocity, of which only the latter moment (determining the doppler bandwidth) is significantly dependent on the principal wind-sea components. However, it should be noted that the theoretical doppler spectra apply to the idealized case of a parallel incident beam. In operation from a moving satellite, the finite beam angle of a real scatterometer would lead to variable doppler shifts due to the platform motion which would normally mask the wave-induced doppler spectrum.

Two courses may be pursued to overcome the limitations of the lowest-order models. Firstly, interrelationships may be established between the accessible high wavenumber range of the spectrum, the wind-sea spectrum and the local surface wind. In this respect it is encouraging that the high-frequency range of the spectrum does not appear to represent a universal equilibrium governed solely by white-capping, but contains a free energy factor governed, among other processes, by the coupling to the principal wind-sea

Table 1

	geometric reflexion	Bragg scattering
Cross section σ	$\dfrac{\exp\{-\phi^2/2\langle n_{/\!/}^2\rangle\}}{2\pi\ \lvert\langle n_\alpha n_\beta\rangle\rvert^{/\!/2}}$	$k_3^4\ T(\phi)\,[F(\underset{\sim}{k}_g)+F(-\underset{\sim}{k}_g)]$
Doppler spectrum $f(\omega)$	$\dfrac{\phi\ \exp\{-\omega^2/8k_3^2\langle u_3^2\rangle\}}{(8\pi k_3^2\langle u_3^2\rangle)^{\frac{1}{2}}}$	$k_3^4 T(\phi)\,[F(\underset{\sim}{k}_g)\,\delta(\omega-\omega_g)+ F(-\underset{\sim}{k}_g)\,\delta(\omega+\omega_g)]$

ϕ = angle of incidence

k_3 = vertical wavenumber component of incident wave

$n_\alpha = \dfrac{\partial\zeta}{\partial x\alpha}$ = wave slope , $\langle n_\alpha n_\beta\rangle = \int F(\underset{\sim}{k})\,k_\alpha k_\beta\,d\underset{\sim}{k}$

$n_{/\!/}$ = wave slope parallel to horizontal direction of incident ray

$\underset{\sim}{k}_g = -2\underset{\sim}{k}_i$ = wavenumber of Bragg scattering surface waves

$\omega_g = (gk_g)^{\frac{1}{2}}$

u_3 = vertical orbital velocity

$\langle u_3^2\rangle = \int F(\underset{\sim}{k})\,gk\,d\underset{\sim}{k}$

components. As pointed out in §5, however, many details of the spectral energy balance at very high wavenumbers still need to be resolved. Several of the inconsistencies in the reported wind dependences of microwave and acoustic cross-sections or in the values of Phillips' constant are presumably due to inadequate consideration of all factors influencing the high-wavenumber equilibrium (cf. [1] [11] [29] [34] [39] [44] [46] [55]).

It has not always been sufficiently appreciated in this context that an observed wind dependence of backscatter cross-sections or Phillips' constant necessarily implies a dependence on further parameters by dimensional arguments alone, independent of detailed dynamical considerations. If the surface-wave spectrum is expressed in terms of a generalised Phillips' form $E_2(f,\theta) = \alpha(f,\theta) g^2 (2\pi)^{-4} f^{-5}$, the non-dimensional form factor α can depend (besides on the non-dimensional direction θ) only on non-dimensional combinations of f and various external parameters such as the wind speed u , the fetch x , and g . Thus if it is assumed that these are the only relevant external variables and α is observed to be independent of f (Phillips' power law), it can be a function only of the non-dimensional combination xg/u^2 (Kitaigorodskii's similarity relation); the determination of wind dependence is meaningful in this case only if the fetch is defined.

For large fetches, α should then attain an asymptotic value independent of wind speed. If a variation of α with wind speed is nevertheless observed for large fetches, this implies either that Phillips' power law is invalid (the wind dependence corresponding in this case to an inverse frequency dependence through the dimensional condition $\alpha = \alpha(uf/g)$, or that additional dimensional factors (e.g. surface tension or contamination) are involved. It follows generally that the wind dependence cannot be investigated consistently without regard to the other parameters which determine the energy level of the wave spectrum at high wavenumbers.

The second, more direct course is to develop higher-order interaction models which predict backscatter signatures dependent not only on the short scattering waves, but also on the longer wind-wave components. Progress in this direction may indeed be a prerequisite for the success of the first approach, for even after the interrelationship between the high-wavenumber energy, the wind-sea spectrum and the wind speed has been clarified, knowledge of the high wavenumber range of the spectrum alone will probably prove insufficient to solve for the remaining two factors determining the equilibrium without additional data on the longer wind-sea components.

8. THE WAVE-FACET INTERACTION MODEL

Two straightforward generalisations of the lowest order scattering models have been investigated. In the first case, the perturbation expansion in terms of surface wave height, which yields Bragg scattering to first order, is extended to quadratic and higher powers. The second order wave-wave interaction theory yields a useful description of backscatter at decameter wavelengths or longer([23] [25] [8]), but is of only limited value in the microwave band, since for short wavelength radiation the principal wind-sea components violate the basic interaction condition (surface wave height)/(electromagnetic wavelength) << 1.

This difficulty is avoided in the composite-wave or wave-facet interaction model, which is based on an alternative two-scale expansion method (cf [9] [10] [49] [57]). In this case the Bragg scattering waves are assumed to be superimposed on a random ensemble of longer carrier waves (the wind sea), which are represented locally by plane facets of dimension small compared with the wind-sea wavelength but large compared with the wavelength of the Bragg waves. It is then assumed that Bragg theory can be applied as before in the local reference system of the moving, inclined facet. Modifications of the Bragg return arise both through changes in the angle of incidence and the orientation of the polarisation planes relative to the local

facet normal (electromagnetic interactions) and through the amplitude and wavelength modulation of the Bragg scattering waves as they propagate through the variable orbital currents and vertical accelerations of the carrier waves (hydrodynamic interactions). The model is meaningful only if these modifications are large compared with the errors incurred through the indeterminacy relations (i.e. the Fraunhofer patterns) in restricting the area of the Bragg scattering waves to a finite facet rather than an infinite plane. The condition may be expressed as $k_3 \zeta >> |$ [25] where k_3 is the vertical wavenumber component of the incident radiation and ζ is the wave height.

Theoretical investigations of the wave-facet model have been restricted hitherto to the electromagnetic interactions. Except for rather low grazing angles (less than about 20°), these are not found to appreciably affect the backscatter cross-sections. Moreover, the modifications are proportional to the mean square wave slopes, which are only weakly dependent on the main part of the wind-sea spectrum. Stronger effects are found in the doppler spectra, the wind-sea signatures here being determined by the mean square orbital velocities and the mean products of the orbital velocities and wave slopes [25], both of which represent spectral moments weighted towards the principal components of the wind-sea spectrum. In prin-

cipal, doppler measurements could therefore yield independent estimates of, say, the mean wave height and mean period of the sea. However, apart from the aforementioned difficulties in resolving wave-induced doppler shifts from satellites, the theoretical predictions must be regarded as qualitative until the hydrodynamic interactions, which are generally of order comparable with the electromagnetic interactions, are incorporated in the model. This would not only be useful for the interpretation of the doppler spectra, but may also enhance the value of cross-section data by the prediction of new types of signatures (such as the upwind/downwind asymmetry, cf. [24]), which may be more readily distinguishable from the unmodulated Bragg return than the modifications induced by electromagnetic interactions alone.

Perhaps the strongest argument for developing a quantitative wave-facet interaction model including both types of interaction is the recent interesting proposal to determine the complete wind-sea spectrum by means of sinusoidally modulated microwaves (Ruck et al, (1972) — a similar suggestion was made also in an earlier unpublished communication by W.S. Ament). The power emitted by a microwave beam consisting of the superposition of two monochromatic waves with closely neighboring frequencies and horizontal wavenumbers ($\omega_1, \underset{\sim}{k}_1$) and ($\omega_2, \underset{\sim}{k}_2$),

respectively, may be represented as a D.C. term and a superimposed sinusoidal modulation at the difference frequency and wavenumber ($\omega_m, \underset{\sim}{k}_m$) = ($\omega_1 - \omega_2, \underset{\sim}{k}_1 - \underset{\sim}{k}_2$). (It is assumed here that the power is averaged over a period large compared with ω_1^{-1} but small compared with ω_m^{-1} .) On account of its finite frequency ω_m , the modulation term can be readily filtered from the mean power. Thus separated, the value of the fluctuating beam as a wave probe follows primarily from its sinusoidal spatial variation. Assuming that the Bragg scattering surface waves were essentially homogeneous over scales large compared with the modulation wavelength $\lambda_m = 2\pi/| \underset{\sim}{k}_1 - \underset{\sim}{k}_2 |$, the modulated backscattered return, integrated over an illuminated area of dimension large compared with λ_m , would average to effectively zero. However, if the Bragg-scattering surface waves are themselves modulated by long wind-sea components, the product of the modulated incident power and the modulated backscatter cross-section yields a non-vanishing contribution on integration over the illuminated area. If the modulation of the Bragg scattering waves is linear with respect to the wind sea, which appears a reasonable first approximation, the modulated microwave acts as a filter extracting the modulating wind-sea component at the wavenumber $\underset{\sim}{k}_m$. Since the effect is linear in the (statistical) surface wave amplitudes, the ensemble average of

the backscattered power at the frequency ω_m would still vanish. (The filter separating the modulated power from the D.C. term must, of course, be sufficiently wide to include the small doppler broadening due to the waves — or the platform motion.) However, the mean square power at ω_m is non-zero and is proportional to the wind-sea energy spectrum at $\underset{\sim}{k}_m$. (It may be noted that this corresponds to a mean fourth product of the signal amplitudes which could not be inferred from mean quadratic quantities — essentially the mean power — and must therefore represent a non-Gaussian effect. In accordance with the Central Limit Theorem it can be shown that for large areas of illumination the modulated term is small compared with the D.C. term, which has Gaussian statistics.)

By varying the difference frequency and azimuth angle, the technique basically provides a measurement of the complete two-dimensional wind-wave spectrum, with the exception of a sign ambiguity in the direction of wave propagation. However, the method is critically dependent on the determination of the coupling coefficients characterising the modulation of the Bragg return by the spectral components of the wind-sea. The electromagnetic contribution to these interactions can be readily calculated, but the hydrodynamic terms are governed by the same long-short wave interactions that arose in discussions of the energy

balance in §§5 and 7. They can be treated formally by the WKBJ method appropriate to the two-scale approximation of the wave-facet model (cf.[24]), but as pointed out above, a basic difficulty of the theory is that a complete analysis requires, among other processes, the inclusion of dissipative losses due to white capping and the regeneration of short waves by wind, both of which are only poorly known. As before, we conclude that significant progress in the determination of sea state from cross-section data requires detailed experiments to clarify the various processes determining the short-wave energy balance.

9. RADAR ALTIMETRY

The analysis of microwave backscatter signals with respect to delay time yields wave information of a basically different nature from that obtained from time-averaged cross-section or doppler data. Thus with the simplest form of signal treatment, altimeters provide a measurement of the mean square wave-height, a basic characteristic of the wave field which was not accessible to direct measurement by CW methods.

On reflection from the sea surface, an initially step-function pulse is transformed to a pulse with the familiar average shape shown in Fig. 9. If the sea surface is almost calm (except for very small slope variations which broaden the average reflection of a unidirectional ray into

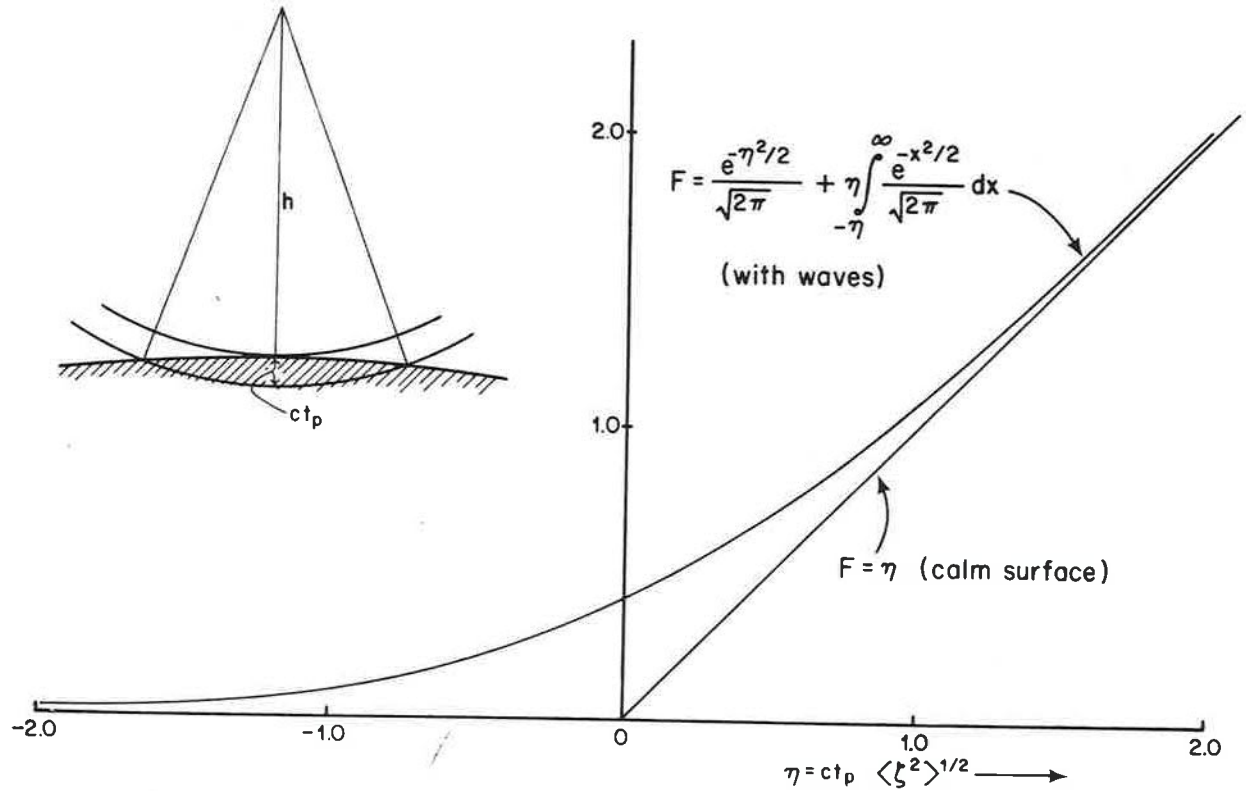

Figure 9. Mean shape (in power) of incident step-function pulse on reflexion from sea surface. The wave field smooths the corner of the linear-ramp response for a calm surface. Solutions for a square pulse are obtained by subtracting a second, identical step-function solution displaced in time.

a narrow but finite angular beam, so that all points within the footprint reflect equal power back to the source) the returned power I at a given delay time $t_d = \frac{2h}{c} + 2t_p$ is proportional to the area of the footprint. For small footprint diameters relative to the source height h, the area increases linearly with the penetration time t_p (cf. Fig. 9), so that

$$I = \begin{cases} 0 \text{ for } t_p \leq 0 \\ \alpha t_p \text{ for } t_p \leq 0 \end{cases} \qquad (3)$$

where the constant α is determined by geometric factors and the mean square wave slope, in accordance with the specular reflexion model valid for normal incidence (cf. table 1). The case of a square-shaped initial pulse follows from the step-function solution (including the modifications considered below) by subtracting a second, identical solution displaced in time.

In the presence of waves, the sharp break at the onset of the reflected pulse is smoothed through the early arrivals of energy reflected from the crests of waves before the pulse reaches the mean sea surface. The modification of the reflected pulse shape contains useful sea state information, but tends also to degrade measurements of the mean sea surface elevation. Particularly important for the latter problem is the question whether the pulse distortion

is indeed limited only to the pulse onset (and the second corner terminating the linear ramp in the square-pulse case) or whether the entire pulse is affected. If the wave signature is restricted to the pulse corners, it can be largely eliminated from the mean surface measurement by extrapolation of the linear regime; if not, a correction must be applied to the entire pulse, and its magnitude can be computed only if the wave field is known.

According to the specular reflexion model, the mean CW power reflected vertically from an infinitesimal area dA is given by

$$dI = \beta P_2(\underset{\sim}{n})_{\underset{\sim}{n}=0} dA \qquad (4)$$

where β is a geometrical constant and $P_2(\underset{\sim}{n})$ the probability distribution of facet slopes $\underset{\sim}{n} = \left(\frac{\delta\zeta}{\delta x_1}, \frac{\delta\zeta}{\delta x_2}\right)$ In the case of a step-function pulse, power is received at the delay time t_d only if the reflecting facet lies within a sphere of radius $R = ct_d/2$. from the source, or in terms of the penetration time t_p and footprint diameter $r = (2hct_p)^{\frac{1}{2}}$, if the surface displacement

$$\zeta \geq \hat{\zeta}(r', t_p) = (r'^2 - r^2)/2h$$

where r' is the radial distance of the element dA from the foot of the surface normal passing through the source. Thus the expression (4) must be replaced in this case by

$$dI = \beta \int_{\zeta}^{\infty} P_3(\zeta, \underset{\sim}{n})\, d\zeta dA$$

where $P_3(\zeta,\underset{\sim}{n})$ is the joint probability distribution of surface slopes and displacements. Integrating over the surface, the backscattered power is thus given by

$$I = \beta\int_0^\infty 2\pi r'\left[\iint_\zeta^\infty P_3(\zeta,\underset{\sim}{n})_{\underset{\sim}{n}=o}\,d\zeta\right]dr' \qquad (5)$$

For a Gaussian wave field, the surface slopes and heights are statistically independent, since

$$\langle\zeta\underset{\sim}{n}\rangle = \langle\zeta\nabla\zeta\rangle = \nabla\langle\zeta^2/_2\rangle = 0$$

on account of the statistical homogeneity. Hence

where $$P_3(\zeta,\underset{\sim}{n}) = P_1(\zeta)P_2(\underset{\sim}{n}) \ ,$$

$$P_1(\zeta) = (2\pi\langle\zeta^2\rangle)^{-\frac{1}{2}}\exp\{-\zeta^2/2\langle\zeta^2\rangle\}$$

Substituting in equation (5), the integrations can be preformed explicitly, yielding

$$I = \alpha\langle\zeta^2\rangle^{\frac{1}{2}}c^{-1}\{(2\pi)^{-\frac{1}{2}}\exp(-\eta^2/_2) + \eta\phi(\eta)\} \qquad (6)$$

where $\eta = ct_p/\langle\zeta^2\rangle^{\frac{1}{2}}$, $\phi(\eta) = \int_\eta^\infty e^{-\eta'^2/2}\,d\eta'$

denotes the error function and α is the same constant as in equation (3).

We note that the shape of the pulse onset shown in Fig. 9 is the same for all sea states, equation (6) depending on the wave field only through the single scaling

parameter $\langle \zeta^2 \rangle$.

A preliminary analysis indicates that further useful parameters of the wind-sea, including wavelength information, can be obtained from a more detailed analysis of the complete doppler spectrum and higher order signal moments. However, the dependence of these functions on the wind-wave spectrum is highly nonlinear, so that the inversion of the functional relations presents a nontrivial mathematical problem which can probably be solved only numerically with the aid of parametrised representations of the wind-wave spectrum.

According to the solution (6), the wave field affects only the onset of the reflected pulse, the asymptotic pulse shape approaching the calm-surface solution (3) (as, of course, must be the case if the solutions for all sea states, including the limit $\langle \zeta^2 \rangle \to 0$, differ only by a scale factor). Although this result appears encouraging for the measurement of mean sea surface, it is a particular consequence of the Gaussian hypothesis, with its corollary of statistically independent wave slopes and surface heights. In the non-Gaussian case, the asymptotic pulse shape is in general parallel to, but offset from, the calm-surface solution. Physically, if the mean square wave slopes tend to be higher on the wave crests than in the troughs, the average energy reflected vertically from the

wave crests is smaller than from the troughs, and the mean backscattered power is biased towards greater delay times. Thus a linear extrapolation of the asymptotic pulse response defines a virtual onset time corresponding to a calm-surface elevation lower than the true mean surface. For significant correlations between the wave height and the wave slope squared the systematic error introduced in this manner could become of the order of the r.m.s. wave height. Although this will normally not exceed the achievable resolution of currently planned space altimeters, it could become serious should the sought-for dm resolution needed for most oceanographic applications (tides, geostrophic surface slopes, wind set up, etc.) become attainable. The correction for these errors will require not only measurements of the wave field but also an understanding of the coupling between the long wind-sea components and the shorter waves contributing to the mean square slope — which is essentially the same two-scale interaction problem that has been mentioned repeatedly above.

10. CONCLUSIONS

Microwave measurements from space hold considerable promise of yielding valuable synoptic data on sea state and surface winds. However, the interaction between microwaves and the surface is highly complex and poses several fundamental questions which require further extensive study

before the techniques can be usefully applied. Investigations are needed particularly in two areas:

(1) A detailed theoretical analysis of the complete doppler spectrum (or scattering function) and the non-Gaussian properties of backscatter signals may be expected to reveal additional useful sea-state signatures not contained in the traditional cross-section, doppler and travel-time measurements. This applies particularly to the backscatter statistics for radar altimeters, which appear to be intimately related to the wind-sea spectrum.

(2) Higher-order models of the radar return from the sea surface are strongly dependent on the interactions between very short waves and the longer wind-sea components. A second basic input for these models is the energy level of the wave spectrum at high wavenumbers. Both questions represent interrelated aspects of the energy balance of the short-wave region of the spectrum, and can be understood only through detailed measurements covering several decades of surface wavelengths from a few cms to several hundred meters. A broad-band wave experiment of this nature, combined with radar backscatter data — supplemented, if possible, by microwave-temperature and acoustic backscatter measurements as independent tests of the theoretical models— would be very helpful in clarifying some of the basic mechanisms involved in the interpretation of microwave backscatter from the sea surface.

REFERENCES

1. Bachmann, W. and B. de Raignac (1971) The calculation of the surface backscattering coefficient of underwater sound from measured data. SACLANTCEN Techn. Mem.No. 174

2. Baer, L. (1963) An experiment in numerical forecast of deep water ocean waves. Lockheed Missile Space Co., LMSC-801296

3. Barnett, T.P. (1968) On the generation, dissipation and prediction of wind waves. J. Geophys. Res. 73, 513-534

4. Barnett, T.P. (1970) Wind waves and swell in the North Sea. EOS 51 544-550

5. Barnett, T.P., E. Bouws, H. Carlson, D. Cartwright, J.A. Ewing, H. Gienapp, D.E. Hasselmann, K. Hasselmann, P. Krusemann, A. Meerburg, K. Richter, W. Sell and H. Walden (1971) Measurements of wind-wave growth and swell decay in the North Sea (Joint North Sea Wave Project - JONSWAP), AGU, Washington, April 1971, and IUGG, Moscow, Aug. 1971 (to be published in Deutsche Hydrogr. Zeitschrift)

6. Barnett, T.P. and J.C. Wilkerson (1967) On the generation of wind waves as inferred from airborne radar measurements of fetch-limited spectra. J. Mar. Res. 25, 292-328

7. Barnett, T.P. and A.J. Sutherland (1968) A note on the overshoot effect in wind-generated waves. J. Geophys. Res. 73, 6879-6884

8. Barrick, D.E. (1971) Dependence of second-order doppler side bands in HF sea echo upon sea state, G-AP Internat. Symp. Digest

9. Barrick, D.E. and W.H. Peake (1968) A review of scattering from surfaces with different roughness scales. Radio Sci. 3, 865-868

10. Bass, F.G., I.M. Fuks, A.I. Kalmykov, I.E. Ostrovsky and A.D. Rosenberg (1968) Very high frequency radiowave scattering by a disturbed sea surface. IEEE Trans., AP-16, 554-568

11. Chapman, R.P. and J.H. Harris (1962) Surface back-scattering strengths measured with explosive sound sources. J. Acoust. Soc. Am. 34, 1592-1597

12. Cox, C.S. and W.H. Munk (1954) Statistics of the sea surface derived from sun glitter. J. Mar. Res. 13, 198-227

13. Cox, C.S. and W.H. Munk (1954b) Measurements of the roughness of the sea surface from photographs of the sun's glitter. J. Optical Soc. Amer. 44, 838-850

14. Davis, R.E. (1969) On the high Reynolds number flow over a wavy boundary. J. Fluid Mech. 36, 337-346

15. Davis, R.E. (1970) On the turbulent flow over a wavy boundary. J. Fluid Mech. 42, 721-731

16. Dobson, F.W. (1971) Measurements of atmospheric pressure on wind-generated sea waves. J. Fluid Mech. 48, 91-127

17. Evans, V.U. and T. Hagfors (1968) Radar astronomy. McGraw Hill Book Co.

18. Ewing, J.A. (1971) Paper on wave prediction - to appear in Deutsche Hydrogr. Zeitschr. 24 (6)

19. Hasselmann, D.E. (1971) Wave generation by resonant Case-mode interactions in a turbulent wind. AGU, Washington, April 1971 (publ. in preparation)

20. Hasselmann, K. On the non-linear energy transfer in a gravity-wave spectrum.

    a. (1962) Part 1: General Theory. J. Fluid Mech. 12, 481-500

    b. (1963) Part 2: Conservation theorems, wave-particle correspondence, irreversibility. J. Fluid Mech. 15, 273-281

    c. (1963) Part 3: Computation of the energy flux and swell-sea interaction for a Neumann spectrum. J. Fluid Mech. 15, 385-398

21. Hasselmann, K. (1967) Nonlinear interactions treated by the methods of theoretical physics (with application to the generation of waves by wind) Proceedings of the Royal Society, A, 299, 77-100

22. Hasselmann, K. (1968) Weak-interaction theory of ocean waves, Basic developments in fluid dynamics (Editor, M. Holt) 2, 117-182

23. Hasselmann, K. (1971) Determination of ocean wave spectra from doppler radio return from the sea surface. Nature 229, 16-17

24. Hasselmann, K. (1971) On the mass and momentum transfer between short gravity waves and larger-scale motions. J. Fluid Mech. 50, 189-206

25. Hasselmann, K. and M. Schieler (1970) Doppler spectra of electromagnetic backscatter from the sea surface at centimeter-decimeter and decameter wavelengths; Proceedings VIIIth Naval Hydrodyn. Symp., Pasadena

26. Kenyon, K.E. (1971) Wave refraction in ocean currents. Deep-Sea Res. 18, 1023-1034

27. Kitaigorodski, S.A. (1962) Applications of the theory of similarity to the analysis of wind-generated wave motion as a stochastic process. Bull. I.Z.V. Geophys. Ser. 1, 73-80

28. Long, R. (1971) On generation of ocean waves by a turbulent wind. Diss., Univ. Miami, 1971

29. Longuet-Higgins, M.S. (1969) A nonlinear mechanism for the generation of sea waves. Proc. Roy. Soc. A. 311, 371-389

30. Longuet-Higgins, M.S. (1969) On wave breaking and the equilibrium spectrum of wind-generated waves. Proc. Roy. Soc. A 310, 151-159

31. Longuet-Higgins, M.S. and R.W. Stewart (1960) Changes in the form of short gravity waves on long waves and tidal currents. J. Fluid Mech. 8, 565-583

32. Longuet-Higgins, M.S. and R.W. Stewart (1961) The changes in amplitude of short gravity waves on steady non-uniform currents. J. Fluid Mech. 10, 529-549

33. Longuet-Higgins, M.S. and R.W. Stewart (1964) Radiation stresses in water waves; a physical discussion, with applications. Deep-Sea Res. 11, 529-562

34. Marsh, H.W. (1963) Sound reflection and scattering from the sea surface. J. Acoust. Soc. Am. 35, 240-244

35. Miles, J.W. (1957) On the generation of surface waves by shear flows. J. Fluid Mech. 3, 185-204

36. Mitsuyasu, H. On the growth of the spectrum of wind-generated waves.

a. (1968) (I) Rep. Research Inst. Appl. Mech., Kyushu Univ. 16, 459-482

b. (1969) (II) Rep. Research Inst. Appl. Mech., Kyushu Univ. 17, 235-248

37. Mitsuyasu, H. (1968) A note on the nonlinear energy transfer in the spectrum of wind-generated waves. Rep. Research Inst. Appl. Mech. Kuyshu Univ. 16, 251-264

38. Mitsuyasu, H., R. Nakayama and T. Komori (1971) Observations of the wind and waves in Hakata Bay. Rep. Research Inst. Appl. Mech. Kyushu Univ. 19, 37-74

39. Moore, R.K., J.P. Claassen, A.K. Fung. S. Wu and H.L. Chan (1971) Toward radscat measurements over the sea and their interpretation. Remote Sensing Lab., Univ.

40. Phillips, O.M. (1957) On the generation of waves by turbulent wind. J. Fluid Mech. 2, 417-445

41. Phillips, O.M. (1958) The equilibrium range in the spectrum of wind-generated waves. J. Fluid Mech. 4, 426-434

42. Phillips, O.M. (1960) On the dynamics of unsteady gravity waves of finite amplitude. Part I. J. Fluid Mech. 9, 193-217

43. Phillips, O.M. (1963) On the attenuation of long gravity waves by short breaking waves. J. Fluid Mech. 16, 321-32

44. Phillips, O.M. (1966) "The Dynamics of the Upper Ocean". Camb. Univ. Press, London and New York

45. Pierson, W.J. (1970) The integration of remote sensing data into global weather prediction, wave forecasting, and ocean circulation computer based systems. New York Univ., NASA-MSC Review

46. Pierson, W.J., F.C. Jackson, R.A. Stacy, and E. Mehr (1971) Research on the problem of the radar return from a wind roughened sea. Contr. No. 117, Geophysic. Sciences Lab., Dept. Met. Ocean., New York Univ., Bronx, N.Y.

47. Pierson, W.J., L.J. Tick and L. Baer (1966) Computer based procedure for preparing global wave forecasts and wind field analysis capable of using wave data obtained by a space craft. 6th Naval Hydrodynamic Symposium, Washington, Office of Naval Res., Washington, D.C.

48. Ruck, G., D. Barrick, T. Kalisvewski (1972) Bistatic radar sea state monitoring. Batelle Tech. Rep., Columbia Lab., Ohio

49. Semenov, B. (1966) An approximate calculation of scattering on the perturbed sea surface. IVUZ Radiofizika (USSR) 9, 876-887

50. Sell, W. and K. Hasselmann (1972) Computations of nonlinear energy transfer for JONSWAP and empirical wind wave spectra. Rep. Inst. Geophysics, Univ. Hamburg

51. Shemdin, O.H. and R.H. Lai (1971) Laboratory investigation of turbulence above waves. IUGG, Moscow, Aug. 1971

52. Snyder, R.L. and C.S. Cox (1966) A field study of the wind generation of ocean waves. J. Mar. Res. 24, 141-178

53. Sutherland, A.J. (1968) Growth of spectral components in a wind-generated wave train. J. Fluid Mech. 33, 545-560

54. Valenzuela, G.R. (1971) Non-linear energy transfer in gravity-capillary wave spectra. AGU Fall Meeting, San Francisco, Dec. 1971 (to be published)

55. Valenzuela, G.R., M.B. Laing and J.C. Daley (1971) Ocean spectra for the high frequency waves as determined from airborne radar measurements. J. Mar. Res. 29, 69-84

56. Valenzuela, G.R. and M.B. Laing (1970) Study of doppler spectra of radar sea echo. J. Geophys. Res. 75, 551-563

57. Wright, J.W. (1968) A new model for sea clutter. IEEE Trans. AP-16, 217-223